Lysine to arginine mutagenesis of chlorotoxin enhances its cellular uptake

Paola G. Ojeda[1,2], Sónia Troeira Henriques[1], Yijun Pan[3], Joseph A. Nicolazzo[3], David J. Craik[1] and Conan K. Wang[1,*]

[1]Institute for Molecular Bioscience, The University of Queensland, Brisbane, Queensland, 4072, Australia; [2]Centro de Bioinformática y Simulación Molecular (CBSM), Universidad de Talca, Talca, Chile; [3]Drug Delivery, Disposition and Dynamics, Monash Institute of Pharmaceutical Sciences, Monash University, Parkville, Victoria, 3052, Australia

*Address correspondence to:

Dr Conan Wang

Institute for Molecular Bioscience,

The University of Queensland,

Brisbane, QLD, 4072, Australia

Tel: 61-7-3346 2014

E-mail: c.wang@imb.uq.edu.au

Keywords: toxin, peptide, disulfide, scorpion venom, cell-penetrating peptide

Funding Source Statement: This work was supported by a grant from the National Health and Medical Research Council of Australia (APP1010552). CKW was supported by an National Health and Medical Research Council Early Career Research Fellowship (546578). DJC is funded by an Australian Research Council Australian Laureate Fellowship (FL150100146). STH is funded by an Australian Research Council Future Fellowship (FT150100398). PGO was supported by Fondo Nacional de Desarollo Científico y Tecnólogico (FONDECYT) grant 3160140.

Abbreviations and Textual Footnotes

CTX	chlorotoxin
CPP	cell-penetrating peptides
kB1	kalata B1
MCoTI-I	*Momordica cochinchinensis* trypsin inhibitor-I
MCoTI-II	*Momordica cochinchinensis* trypsin inhibitor-II
SPR	surface plasmon resonance
Fmoc	fluorenylmethyloxycarbonyl
SPPS	solid-phase peptide synthesis
RP-HPLC	reversed-phase high-performance liquid chromatography
NMR	nuclear magnetic resonance (NMR)
LC-MS	liquid chromatography-mass spectrometry
HeLa	human cervical carcinoma cells
DMEM	Dulbecco's Modified Eagle Medium
FBS	fetal bovine serum
MTT	(3-(4,5-dimethylthiazol-2-yl)-2,5-diphenyltetrazolium bromide)
PBS	phosphate buffered saline
TB	trypan blue
POPC	1-palmitoyl-2-oleoylphosphatidylcholine
POPS	1-palmitoyl-2-oleoylphosphatidylserine
SUB	Small unilamellar vesicle
TOCSY	Total Correlation Spectroscopy
NOESY	Nuclear Overhauser Effect Spectroscopy

Abstract

Chlorotoxin (CTX), a disulfide-rich peptide from the scorpion *Leiurus quinquestriatus*, has several promising biopharmaceutical properties, including preferential affinity for certain cancer cells, high serum stability, and cell penetration. These properties underpin its potential for use as a drug design scaffold, especially for the treatment of cancer; indeed, several analogues of CTX have reached clinical trials. Here, we focus on its ability to internalize into cells – a trait associated with a privileged sub-class of peptides called cell-penetrating peptides – and whether it can be improved through conservative substitutions. Mutants of CTX were made using solid-phase peptide synthesis and internalization into human cervical carcinoma (HeLa) cells was monitored by fluorescence and confocal microscopy. CTX_M1 (i.e. [K15R/K23R]CTX) and CTX_M2 (i.e. [K15R/K23R/Y29W]CTX) mutants showed at least a 2-fold improvement in uptake compared to CTX. We further showed that these mutants internalize into HeLa cells largely via an energy-dependent mechanism. Importantly, the mutants have high stability, remaining intact in serum for over 24 h; thus, retaining the characteristic stability of their parent peptide. Overall, we have shown that simple conservative substitutions can enhance the cellular uptake of CTX, suggesting that such type of mutations might be useful for improving uptake of other peptide toxins.

Cell-penetrating peptides (CPPs) are able to traverse biological membranes and have broad utility in drug delivery.[1-3] The mechanism by which these peptides are internalized into cells varies, but appears to be influenced by their structural and chemical features (e.g. amino acid composition) and the cell membrane properties of their target cell (e.g. lipid and membrane protein composition).[4-7] Specifically, CPPs generally have a high content of positively charged amino acids, such as lysine or arginine, and/or display patches of hydrophobic amino acids that are required for internalization.[8]

CPPs have been used successfully as tools to deliver drugs into cells. Some advantages of CPPs are low toxicity, the ability to be internalized by different types of cells, and the ability to deliver a wide range of cargoes,[9] including nucleic acids,[10-11] nanoparticles[12] and small molecules.[13] For instance, TAT, one of the most widely studied CPPs, has been used to deliver doxorubicin (an anticancer drug) to human ovarian carcinoma cells[14] and to deliver peptide-blockers of c-Jun NH2-terminal kinase to intracellular compartments to block β-cell apoptosis.[15] However, CPPs have some disadvantages, including poor stability in biological systems, which can limit their uptake.[16]

Disulfide-rich peptides are typically very stable and have compact structures. Several disulfide-rich peptides, including those derived from plants and animal venoms, have been reported to be internalized by cells and have been classified as CPPs.[17-19] For example, the plant-derived cyclotides kalata B1 (kB1) and *Momordica cochinchinensis* trypsin inhibitors I and II (MCoTI-I and MCoTI-II), as well as their analogues, have been shown to enter mammalian cells and have been proposed to be promising scaffolds not only for stabilizing bioactive peptides but also for

drug delivery.[19-22] Examples of venom-derived CPPs include crotamine, from the South American Rattlesnake, which shows nuclear localization after being internalized by cells,[23] and maurocalcine, from the venom of the scorpion *Scorpio maurus palmatus*, which binds to the intracellular ryanodine receptor and triggers internal Ca^{2+} release seconds after being applied extracellularly.[17, 24-25]

Another venom-derived disulfide-rich CPP is the 36-amino acid peptide chlorotoxin (CTX),[26] from the Israeli scorpion *Leiurus quinquestriatus* **(Figure 1)**.[27] CTX is particularly well-known as a ligand for targeting cancer cells, which has led to its development into imaging probes that can distinguish tumorigenic from non-tumorigenic tissue.[28-29] 'Tumor paint', an analogue of CTX conjugated to the fluorescent dye Cy5.5™, is one such imaging agent.[29] CTX and CTX-conjugated nanoparticles have also been used as vehicles to deliver drugs and therapeutic macromolecules (e.g. DNA, siRNA) selectively to cancer cells.[30] Despite widespread interest in CTX for its ability to bind preferentially to cancer cells,[28-36] relatively little is known about its ability to penetrate cells – a desirable pharmaceutical trait that could be utilized in drug development. Fundamental questions that currently remain unanswered include the extent of CTX uptake compared to other CPPs and whether its internalization is a property that can be tuned.

In this study, CTX and two analogues (CTX_M1 and CTX_M2) were synthesized and used to examine the effect of increasing the number of arginine and tryptophan residues on cellular uptake. These mutations, although conservative in nature, have been shown to affect, and in some cases, substantially improve cellular uptake of peptides.[37-42] For example, we recently

showed that mutation of both K9 and K10 to arginine residues resulted in a 2-fold enhancement in cellular uptake of MCoTI-II.[43] In the current study, CTX analogues were labeled with either Alexa Fluor® 488 or Cy5.5™ and their internalization by HeLa cells examined using flow cytometry and confocal microscopy. In addition, the ability of the analogues to bind model lipid membranes was measured using surface plasmon resonance (SPR). Our findings suggest that internalization of CTX can be improved by increasing the arginine, and to a lesser extent tryptophan, content. The amount of peptide able to be internalized is also affected by the attached fluorescent dye. Finally, internalization of CTX and its analogues is mediated largely by an energy-dependent mechanism. Understanding the cell-penetrating ability of CTX, including by defining the roles of specific residues, could enable future applications of CTX as a delivery scaffold.

Experimental Procedures

Synthesis and purification

CTX and analogues were synthesized on a Symphony Multiplex automated synthesizer using N-(9-fluorenyl)methyloxycarbonyl (Fmoc) solid-phase peptide synthesis (SPPS) chemistry and purified.[44] After assembly, linear protected peptides were cleaved from the resin using 95:2.5:2.5 TFA/TIPS (triisopropylsilane)/water. The Cys-reduced peptides were purified using C18 columns by reversed-phase high performance liquid chromatography (RP-HPLC), as described previously. Briefly, a linear gradient of Buffer B (90% v/v CH_3CN; 9.95% v/v H_2O; 0.05% v/v CF_3COOH) was mixed with Buffer A (99.95% v/v H_2O; 0.05% CF_3COOH) at 8 mL/min flow rate.

Folding, purification and structural analysis

Reduced CTX at 0.1 mg/mL was oxidized in a buffer containing 0.1 M Tris-HCl pH 7.8, 0.2 M NaCl, 5 mM reduced glutathione and 0.5 mM oxidized glutathione for 16–20 h at room temperature. CTX analogues were oxidized in the same buffer with the addition of 15% (v/v) isopropanol. The oxidized peptides were purified using RP-HPLC at either a 3 mL/min or 8 mL/min flow rate depending on the column. The structures of folded peptides were confirmed using ^1H nuclear magnetic resonance (NMR) spectroscopy, as described previously.[45] Briefly, peptides were dissolved in H_2O/D_2O (9:1, v/v). To determine the chemical shifts of the peptides, NMR spectra were recorded on a Bruker Avance-600 MHz NMR spectrometer at 298 K. The mixing time was 80 ms and 200 ms for TOCSY and NOESY experiments, respectively. Spectra were internally referenced to 2,2-dimethyl-2-silapentane-5-sulfonic acid (DSS) at 0.00 ppm.

Cy5.5™ labeling

CTX and analogues were labeled with Cy5.5™ (GE Healthcare). Peptides at 1 mg/mL dissolved in 0.1 M sodium carbonate pH 9.3 (1 mL) were added to one vial of dye and incubated at room temperature for 3 h. The labeled and unlabeled peptides were separated using RP-HPLC. Purity of monolabeled peptide was confirmed by analytical RP-HPLC and liquid chromatography-mass spectrometry (LC-MS). The peptide concentration was determined by measuring the absorbance at 678 nm (ε_{678}=250000 M^{-1} cm^{-1}). Peptide stocks (TAT, TAT-N, CTX and CTX_M1) were dissolved in water or with the addition of 5% v/v dimethyl sulfoxide (CTX_M2), before being stored at -20°C until use.

Alexa Fluor® 488 labeling

CTX and analogues were labeled with Alexa Fluor® 488, as described previously.[43] Briefly, peptide dissolved in 0.1 M sodium bicarbonate buffer (pH 8.0) was incubated with 2 mol equivalent of Alexa Fluor® 488 (Life Technologies) for 3 h at room temperature. Then, labeled and unlabeled peptides were separated using RP-HPLC. The purity of the monolabeled peptide was confirmed by analytical RP-HPLC and LC-MS. The concentration of the monolabeled peptides was determined by measuring their absorbance at 495 nm (A_{495}) and considering the molar extinction coefficient of Alexa Fluor® 488 at 495 nm (ε_{495}) as 71000 M^{-1} cm^{-1}. Peptides were dissolved in water (TAT, TAT-N, CTX and CTX_M1) or with the addition of 5% v/v dimethyl sulfoxide (CTX_M2), before being stored at -20°C.

Cell culture

Human cervical carcinoma cells (HeLa) were grown in Dulbecco's Modified Eagle Medium (DMEM) supplemented with 10% fetal bovine serum (FBS). Cells were supplemented with 1% (v/v) antibiotic/antimitotic and incubated at 37ºC with 5% CO_2. hCMEC/D3 cells were a generous gift from Pierre-Olivier Couraud (INSERM, France). hCMEC/D3 cells were maintained at 37 ºC in a humidified incubator (5% CO_2/95% O_2) in endothelial basal medium-2 supplemented with vascular endothelial growth factor (0.025% v/v), insulin-like growth factor 1 (0.025% v/v), epidermal growth factor (0.025% v/v), basic fibroblast growth factor (0.1% v/v), hydrocortisone (0.01% v/v), ascorbic acid (0.01% v/v), FBS (0.1% v/v), HEPES (1M, pH 7.4, 1% v/v) and penicillin-streptomycin (1% v/v). The cells were seeded at 50,000 cells/cm^2 onto culture flasks/plates coated with rat tail collagen type I.

Cytotoxicity assay

The cytotoxicity of native CTX and its analogues was measured and analyzed as described previously.[44] In brief, we used the transformation of MTT (3-(4,5-dimethylthiazol-2-yl)-2,5-diphenyltetrazolium bromide) to insoluble formazan crystals by metabolic active cells as a means of detecting cell viability. The insoluble crystals were solubilized using dimethyl sulfoxide and the absorbance (A_{570}) read using a spectrophotometer; the resulting absorbance was directly proportional to the number of living cells per well. To evaluate the toxic effect of CTX and analogues, each peptide was incubated with 10^3 HeLa cells for 2 h using concentrations ranging from 0 to 50 µM. Triton X-100 at 0.01% (v/v) was used as a positive control.

Serum stability

The stability of peptides was examined using a modified version of a previously described protocol.[22] Human male serum (Sigma-Aldrich) was centrifuged at 13,000 rpm for 10 min to remove lipids, and the supernatant was collected and incubated at 37°C for at least 10 min. The reaction was initiated by the addition of the peptide to the serum to a final peptide concentration of 20 µM. The incubation time points were 0, 2, 6, 12 and 24 h. Controls in phosphate buffered saline (PBS) were included. The reaction was stopped by denaturing the serum proteins with urea at a final concentration of 3 M at 4°C for 10 min, followed by the addition of trichloroacetic acid (final concentration of 7% v/v) and incubation at 4°C for 10 min to precipitate serum proteins. For each sample, the supernatant was collected after a 10-min centrifugation at 13,000 rpm, and subsequently analyzed using analytical RP-HPLC with a 2%/min gradient of 90% (v/v) acetonitrile, 9.95% (v/v) water and 0.05% (v/v) trifluoroacetic acid. Triplicates were performed for each experiment.

Flow cytometry analysis

A BD FACSCanto II flow cytometer was used to quantify the fluorescence of Alexa Fluor® 488 (488 nm excitation laser and 530/30 band-pass filter) and Cy5.5 (633 nm excitation laser, 780/60 band-pass filter). HeLa cells or hCMEC/D3 cells were seeded in a 24-well plate (10^5 cells/well) 1 day before the assay. Cells were pre-incubated with CTX or analogues (6 µM) for 1 h at either 4°C or 37°C, followed by washing with cold PBS. The cells were then trypsinized and the cell pellet resuspended in 500 µL of cold PBS, as described previously.[43, 46] Using a cytometer, the mean fluorescence emission of 10,000 cells was measured before and after the addition of 160 µg/mL of trypan blue (TB) for Alexa Fluor® 488-labeled peptides.

Confocal microscopy

The internalization of conjugated peptides was measured in live cells using a confocal microscope. The day before confocal microscopy was performed, 6×10^4 cells/well were seeded in an 8-well coverglass plate. Then, incubated with 6 µM of conjugated peptide for 1 h at either 4°C or 37°C. Following incubation, live cell images were captured at room temperature using an inverted LSM 510 (Zeiss) confocal laser scanning microscope, and subsequently analyzed using ImageJ software.

SPR analysis

SPR experiments were conducted at room temperature with a L1 biosensor chip in a Biacore 3000, as described previously.[47-48] Synthetic lipids 1-palmitoyl-2-oleoylphosphatidylcholine (POPC) and 1-palmitoyl-2-oleoylphosphatidylserine (POPS) obtained from Avanti Polar Lipids were used to prepare model membranes. Small unilamellar vesicles (SUVs) with a diameter of 50 nm and composed of POPC or POPC/POPS (4:1 molar ratio) were obtained by freeze-thaw and sized by extrusion, following previously described protocols.[49] SUVs were deposited onto the L1 chip surface and CTX and its analogues were analyzed for their membrane-binding affinities to POPC and POPC/POPS (4:1) lipid bilayers, as described previously.[47] Peptide and SUV samples were prepared in running buffer (10 mM HEPES containing 150 mM NaCl, pH 7.4). Peptide affinity for synthetic bilayers was analyzed as described previously.[47]

Results

Peptide design, structural characterization and labeling

Electrostatic interactions between basic amino acids in CPPs and negatively charged molecules at the surface of cell membranes have been recognized as important for the uptake of positively charged CPPs. Furthermore, arginine residues seem to favor the internalization of peptides compared to lysine residues.[37-39] CTX has three lysine (K15, 23 and 27) and three arginine residues (R14, 25 and 36) in its sequence. To improve the uptake of CTX, K15 and K23 were replaced with arginine residues. The side chain of K27 in CTX was not modified in any of the analogues to allow for amine-coupled conjugation of the fluorescent probe required for the internalization assay. K27 was selected as the conjugation site based on a previous study of an optimized analogue of CTX for tumor imaging and targeted therapy.[45] The importance of amino acids with hydrophobic side chains in CPPs has been reported,[40-42] thus tryptophan was also incorporated in the CTX sequence (Y29W). Y29 was chosen as the mutation site because of its structural similarity to Trp. The sequences of CTX and two analogues used in this study, as well as their disulfide bond connectivities are shown in **Figure 1B.**

The various peptides were synthesized using SPPS chemistry, folded and then purified using RP-HPLC. The structures of pure CTX and its analogues were characterized using ^{1}H NMR spectroscopy. Total correlation spectroscopy (TOCSY) and nuclear Overhauser effect spectroscopy (NOESY) spectra were recorded at 600 MHz at 298 K and sequence-specific assignments were obtained. Based on the αH NMR chemical shifts, we found that CTX and its analogues have similar overall three-dimensional structures **(Figure 2A)**, confirming that the substitutions did not have an effect on the tertiary structure.

The peptides were labeled with either the dye Alexa Fluor® 488[43] or the near-infrared dye Cy5.5™[29] to allow their internalization by HeLa cells to be monitored. Only pure monolabeled peptides were used, with their identity and purity confirmed by analytical RP-HPLC and LC-MS.

Stability of peptides

CTX is a very stable peptide that can resist enzymatic proteolysis *in vitro* and *in vivo*.[45] To compare the relative stabilities of CTX and its analogues, peptides were incubated in human serum containing proteolytic enzymes and in PBS at 37°C, and monitored over time. As expected, PBS did not have an effect on peptide stability (data not shown). A version of CTX without disulfide bonds but with all cysteines replaced with L-α-aminobutyric acid (Abu)[44] was also included as a control, representing a peptide that degrades rapidly in serum. Consistent with previous studies,[44-45] CTX was highly stable, with around 90% of intact peptide remaining after 24 h of incubation, and the disulfide-bond deleted analogue of CTX was degraded in less than 4 h **(Figure 2B)**. CTX analogues showed levels of stability similar to that of CTX **(Figure 2B)**.

Cytotoxicity analysis

Cytotoxicity of the compounds was assessed to determine a suitable working peptide concentration for our internalization studies. Although CTX has been reported to be non-toxic to mammalian cells,[44, 50] in the present study cell viability was tested to investigate whether the replacement of lysine and tyrosine residues affects the cytotoxicity of CTX analogues. Neither CTX nor its analogues were cytotoxic to HeLa cells up to a peptide concentration of 50 μM, as shown in **Figure 2C**.

Internalization of CTX and analogues labeled with Alexa Fluor® 488 and Cy5.5™

Quantification of cellular uptake was investigated using fluorophore-labeled peptides. The experiments were performed with HeLa cells at 4°C and 37°C, and the fluorescence emissions of Alexa Fluor® 488 and Cy5.5™ were measured using flow cytometry. As in a previous study,[43] two short peptides were used as controls: TAT (YGRKKRRQRRRPPQG-amide), a 14-mer derived from the region of the HIV-1 Tat protein, which is known for its ability to penetrate cellular membranes; and, TAT-N (YGGGKGGQGGGPPQG-amide), in which all cationic residues from the TAT peptide were replaced with glycine, with the exception of K5 (which was preserved to enable conjugation to the fluorophore). TAT-N was used as a measure of poor internalization by HeLa cells. **Figure 3** shows a clear difference in terms of the uptake ratio between TAT and TAT-N, supporting the use of these peptides as controls for high and low uptake, respectively. A fixed concentration of 6 μM was used to compare internalization of peptides after a 1-h incubation.

Figure 3A shows the internalization of peptides labeled with Alexa Fluor® 488 at 37°C. CTX was able to enter cells but to a similar extent as TAT-N, which was used as a marker of poor cellular uptake. The introduction of two arginine residues into the sequence of CTX (CTX_M1) improved cellular uptake by approximately 2-fold. However, the introduction of an additional tryptophan residue (CTX_M2) did not further improve internalization, as the internalization rate is similar to CTX_M1, suggesting that the two arginine residues introduced into the sequence have the greatest effect on cell uptake of CTX. To evaluate whether the differences in uptake ratio were due to membrane binding, the intensities of the fluorescence reading before and after

adding trypan blue (a membrane-impermeable quencher) were measured. No significant differences in uptake in HeLa cells were observed before and after adding trypan blue (data not shown), suggesting that CTX or its analogues were not bound to the cellular membrane. We also determined the uptake of CTX and its analogues in hCMEC/D3 cells, which unlike HeLa cells, are endothelial in nature but are interesting because they are commonly used to mimic the human blood-brain barrier.[51] As shown in Supplementary Figure S1, the relative uptake of CTX and its analogues compared to TAT and TAT-N are similar in hCMEC/D3 cells and HeLa cells, suggesting that the uptake efficiencies of CTX_M1 and CTX_M2 relative to CTX might be shared between epithelial and endothelial cells.

Figure 3B shows the internalization of peptide labeled with Cy5.5™ at 37°C by HeLa cells. CTX labeled with Cy5.5™ showed an improved ratio of internalization compared to TAT-N. CTX_M1 showed improved internalization by about 80% compared to CTX and the introduction of tryptophan (CTX_M2) also improved internalization, with uptake that was 80% that of TAT. In this case we could not use trypan blue to determine whether peptide membrane binding contributed to the observed fluorescence because trypan blue absorbs light at a similar wavelength as Cy5.5™.

Internalization of CTX and its analogues was examined at 4°C. At 4°C all energy-dependent internalization processes are inhibited or slowed and the lipid bilayer exhibits increased rigidity. **Figures 3C** and **D** show the internalization of peptides labeled with Alexa Fluor® 488 and Cy5.5™ at 4°C, respectively. Apart from TAT labeled with Alexa Fluor® 488, which was able

to enter cells at 4°C, the other peptides were unable to penetrate cells to any significant degree at the lower temperature.

Peptides were observed using confocal microscopy of live HeLa cells to confirm internalization. **Figure 4** shows CTX, CTX_M1 and CTX_M2 labeled with Alexa Fluor® 488 and Cy5.5™ after a 1-h incubation at 37°C. The internalized peptides display a punctate distribution inside cells, consistent with endosomal localization, and no fluorescence was detected when the internalization experiments were performed at 4°C (data not shown). This result confirms our data obtained using FACS, and supports the hypothesis that the CTX peptides are internalized by cells and not restricted to the cell membrane.

Membrane binding studies using SPR

Interaction with lipids of cell membranes has been reported to be an important step in the internalization of some CPPs.[20, 52] We were interested in the contribution of lipid binding to the cellular uptake of CTX and its analogues. Mammalian cell membranes have a fluid and neutral outer leaflet in which phospholipids containing a phosphatidylcholine (PC)-head group are most abundant; therefore, POPC phospholipid, which forms bilayers with a fluid phase at room temperature, was used to mimic the neutral charge and the fluid phase characteristic of these membranes. Negatively charged phosphatidylserine (PS)-containing phospholipids are also present in mammalian cells, and are more abundant in cancerous cell membranes than in normal cells. Thus, to evaluate if electrostatic attractions between the lipid membrane and positively charged peptides are important, the binding of the CTX peptides to lipid bilayers composed of POPC/POPS (80:20) was also studied by SPR using a L1 chip. This method monitors peptide

binding to lipid bilayers in real time. Concentrations up to 200 μM of CTX or analogues were used. Although **Figures 5A, B and C** show peptide binding to lipids (POPC) increases with higher peptide concentration, importantly the amount of peptide bound, as indicated by the peptide to lipid ratio, is low. Specifically, when the membrane affinities of CTX and analogues are compared with the affinities of other peptides that we have previously characterized, for example kalata B1 or TAT,[20, 47] the affinity of CTX and its analogues to the tested lipid bilayers is low. The same trend was observed when the POPC/POPS lipid system was used (data not shown). These results suggest that direct binding to POPC or POPS lipids plays a minor role in the uptake of CTX and its analogues.

To examine whether Alexa Fluor® 488 and Cy5.5™ play a role in the lipid-binding properties of CTX and CTX_M1, labeled and unlabeled peptides (25 μM) were compared on their ability to bind to POPC/POPS membranes. **Figure 6A** shows the binding of unlabeled peptides and peptides labeled with Alexa Fluor® 488 to POPC/POPS membranes. The results show a slight difference between labeled and unlabeled peptides, suggesting that this dye might have a small effect on the binding of the peptides to negatively charged membranes. As shown in **Figure 6B,** Cy5.5™ causes a 2-fold and 3-fold increase in the binding of CTX and CTX_M1, respectively, to POPC/POPS membranes compared to the unlabeled peptides. The difference between Alexa Fluor® 488- and Cy5.5™-labeled peptides is also observed for the internalization of peptides into HeLa cells, supporting the hypothesis that the dye used to investigate CPP uptake can modify their properties.

Discussion

The aim of this work was to investigate the cell-penetrating properties of CTX. In particular, we were interested in the effect of conservative substitutions of lysine to arginine as well as tyrosine to tryptophan. Our results show that the cellular uptake of CTX can be improved by replacing two lysine residues with arginine residues, and that these substitutions do not affect the stability or structure of CTX. This knowledge can guide further molecular optimization of the cell-penetrating properties of CTX. Furthermore, the arginine-rich version of CTX has the potential to be used as a scaffold to deliver compounds selectively to, and then into, cancer cells.

We found that replacing two lysine residues (K15 and K23) with arginine residues increased the internalization of CTX 2-fold. Arginine residues are believed to facilitate cellular uptake of a parent peptide because their guanidinium cationic group can potentially form favorable interactions with surface-exposed components at the cell surface (via interactions with lipids, membrane proteins, etc).[37-38, 53-55] Indeed, polyarginine peptides represent the simplest CPPs and have been used to deliver molecules intracellularly.[56] Our finding that CTX can be modified by introducing arginines into its sequence, resulting in a more effective CPP, provides further confirmation that arginine residues are important facilitators of cellular uptake. In addition to positively charged residues, tryptophan has been shown to affect membrane translocation;[40-42] however, we found that the incorporation of a tryptophan residue at position 29 did not further enhance internalization of CTX_M1. This result is consistent with previous studies showing that both the positions of the tryptophan residues and the size of the hydrophobic patch they form affect cellular uptake efficiency.[41] Additionally, we showed that the fluorescent dye used to investigate the mechanisms of cellular uptake and intracellular distribution of CTX can affect its

cell-penetration properties. This result is consistent with previous reports showing that the labels and cargoes attached to a CPP affect its localization and internalization.[57-63] In our case, although the uptake of CTX and its analogues relative to one another is independent of the dye used (i.e. CTX < CTX_M1 ~ CTX_M2), the internalization of the peptides attached to Cy5.5™ is greater than that of their respective counterparts attached to Alexa Fluor® 488.

Using two different temperatures (i.e. 4°C and 37°C), we observed that CTX and its analogues can be internalized by HeLa cells only at physiological temperature, suggesting that CTX enters cells via endocytosis – a receptor-mediated energy-dependent mechanism. This result is consistent with a previous study showing that radiolabeled CTX could enter D54 MG cells, which are human glioma cells, at 37°C but not 4°C.[64] From the confocal images we observed that CTX and analogues have a punctate pattern of cellular distribution, suggesting that they follow an endocytic pathway after being internalized by HeLa cells. Furthermore, since CTX affinity for synthetic POPC and POPS lipids is low compared to other membrane binding peptides,[24, 51] we hypothesize that CTX is carried into cells by other membrane components.

CTX has several promising biopharmaceutical properties that underpin its potential as a drug design scaffold. One of these properties that has perhaps attracted the most interest from medicinal chemists is the ability to specifically target cancer cells, which has led to the development of CTX into imaging probes that can distinguish tumorigenic from non-tumorigenic tissue.[28-29] Additionally, CTX is very stable (unlike peptides in general), a property that is retained by the improved arginine-rich CTX reported here. As CTX can also internalize into cells, we speculate that it represents a promising scaffold for the design of drugs that target

intracellular proteins for the treatment of a wide range of diseases including cancer. Interestingly, it was recently shown that the disulfide-rich peptide MCoTI-II could be re-designed to exhibit cellular uptake efficiency, comparable to that of TAT, by incorporating more drastic changes to its sequence[22] than those applied in this study, suggesting that further improvements to the cell-penetrating properties of CTX are possible.

Although CTX has several promising biopharmaceutical properties, it also has limitations (which are typical of peptides in general[65-66]) that could restrict its therapeutic potential for now. For example, despite being taken up by cells, it appears that the majority of internalized CTX is trapped inside endosomes, restricting its delivery into the cytoplasm. Many other cell-penetrating peptides have also been reported to have this limitation, which is a major obstacle for peptide-mediated intracellular drug delivery.[67] Encouragingly, recent studies have shown that cell-penetrating peptides can be modified to help them escape from endosomes; [67-68] thus, it might be possible to modify CTX to increase the cytosolic concentration after cellular uptake. Another limitation of peptides, including CTX,[29, 69] is poor *in vivo* half-life due to rapid renal clearance (molecules <30 kDa are excreted rapidly by glomerular filtration). There are now several strategies available to overcome this limitation, including conjugation to polyethylene glycol or affinity tags that bind serum proteins, which have been successful in enhancing *in vivo* half-life.[70-71] For example, liraglutide (marketed as Victoza®), which is used for treatment of type II diabetes or obesity, is an analog of the GLP-1 peptide. Compared to the parent compound, it contains an attached fatty acid molecule that increases it binding to serum albumin, resulting in slower degradation and reduced renal elimination.

Conclusion

Here, we showed that cellular uptake of CTX could be improved by tuning its sequence – specifically by replacement of lysine with arginine residues. This mutagenesis strategy is conservative in nature and could, in principle, be applied to improve uptake of other toxins. In some cases, a conservative mutagenesis strategy is desirable to minimize effects on other properties of the parent peptide. Indeed, the analogues presented herein retained the structure, low toxicity and stability of CTX. Looking beyond CTX, there are many venom-derived peptides that have been recently reported to have high sequence similarity to CTX.[72] These chlorotoxin-like peptides might also serve as tuneable drug design scaffolds with potential for use in drug delivery.

Acknowledgements

We acknowledge the facilities, and the scientific and technical assistance of the Queensland NMR Network. The authors thank Ashley Cooper for editorial assistance.

Supporting Information Available

Internalization of CTX and its analogues by hCMEC/D3 cells is provided in the supporting information.

References

1. Lonn, P.; Dowdy, S. F., Expert Opin. Drug Deliv. 2015, 12, 1627-36.

2. Medina, S. H.; Miller, S. E.; Keim, A. I.; Gorka, A. P.; Schnermann, M. J.; Schneider, J. P., Angew. Chem. Int. Ed. Engl. 2016, 55, 3369-72.

3. Henriques, S. T.; Melo, M. N.; Castanho, M. A., Biochem. J. 2006, 399, 1-7.

4. Di Pisa, M.; Chassaing, G.; Swiecicki, J. M., Biochemistry 2015, 54, 194-207.

5. Sharmin, S.; Islam, M. Z.; Karal, M. A.; Alam Shibly, S. U.; Dohra, H.; Yamazaki, M., Biochemistry 2016, 55, 4154-65.

6. Duchardt, F.; Fotin-Mleczek, M.; Schwarz, H.; Fischer, R.; Brock, R., Traffic 2007, 8, 848-66.

7. Futaki, S.; Nakase, I.; Tadokoro, A.; Takeuchi, T.; Jones, A. T., Biochem. Soc. Trans. 2007, 35, 784-7.

8. Takayama, K.; Hirose, H.; Tanaka, G.; Pujals, S.; Katayama, S.; Nakase, I.; Futaki, S., Mol. Pharm. 2012, 9, 1222-30.

9. Copolovici, D. M.; Langel, K.; Eriste, E.; Langel, U., ACS Nano. 2014, 8, 1972-94.

10. Meade, B. R.; Dowdy, S. F., Adv. Drug Deliv. Rev. 2008, 60, 530-6.

11. Jafari, M.; Karunaratne, D. N.; Sweeting, C. M.; Chen, P., Biochemistry 2013, 52, 3428-35.

12. Gupta, B.; Levchenko, T. S.; Torchilin, V. P., Adv. Drug Deliv. Rev. 2005, 57, 637-51.

13. Lindgren, M.; Rosenthal-Aizman, K.; Saar, K.; Eiriksdottir, E.; Jiang, Y.; Sassian, M.; Ostlund, P.; Hallbrink, M.; Langel, U., Biochem. Pharmacol. 2006, 71, 416-25.

14. Nori, A.; Jensen, K. D.; Tijerina, M.; Kopeckova, P.; Kopecek, J., Bioconjug. Chem. 2003, 14, 44-50.

15. Bonny, C.; Oberson, A.; Negri, S.; Sauser, C.; Schorderet, D. F., Diabetes 2001, 50, 77-82.

16. Palm, C.; Jayamanne, M.; Kjellander, M.; Hallbrink, M., Biochim. Biophys. Acta. 2007, 1768, 1769-76.

17. Boisseau, S.; Mabrouk, K.; Ram, N.; Garmy, N.; Collin, V.; Tadmouri, A.; Mikati, M.; Sabatier, J. M.; Ronjat, M.; Fantini, J.; De Waard, M., Biochim. Biophys. Acta. 2006, 1758, 308-19.

18. Radis-Baptista, G.; Kerkis, I., Curr. Pharm. Des. 2011, 17, 4351-61.

19. Cascales, L.; Henriques, S. T.; Kerr, M. C.; Huang, Y. H.; Sweet, M. J.; Daly, N. L.; Craik, D. J., J. Biol. Chem. 2011, 286, 36932-43.

20. Henriques, S. T.; Huang, Y. H.; Chaousis, S.; Sani, M. A.; Poth, A. G.; Separovic, F.; Craik, D. J., Chem. Biol. 2015, 22, 1087-97.

21. Ji, Y.; Majumder, S.; Millard, M.; Borra, R.; Bi, T.; Elnagar, A. Y.; Neamati, N.; Shekhtman, A.; Camarero, J. A., J. Am. Chem. Soc. 2013, 135, 11623-33.

22. Huang, Y. H.; Chaousis, S.; Cheneval, O.; Craik, D. J.; Henriques, S. T., Front. Pharmacol. 2015, 6, 17.

23. Kerkis, A.; Kerkis, I.; Radis-Baptista, G.; Oliveira, E. B.; Vianna-Morgante, A. M.; Pereira, L. V.; Yamane, T., FASEB J. 2004, 18, 1407-9.

24. Tisseyre, C.; Ahmadi, M.; Bacot, S.; Dardevet, L.; Perret, P.; Ronjat, M.; Fagret, D.; Usson, Y.; Ghezzi, C.; De Waard, M., Biochim. Biophys. Acta. 2014, 1843, 2356-64.

25. Ronjat, M.; Feng, W.; Dardevet, L.; Dong, Y.; Al Khoury, S.; Chatelain, F. C.; Vialla, V.; Chahboun, S.; Lesage, F.; Darbon, H.; Pessah, I. N.; De Waard, M., Proc. Natl. Acad. Sci. U. S. A. 2016, 113, E2460-8.

26. Wiranowska, M.; Colina, L. O.; Johnson, J. O., Cancer Cell. Int. 2011, 11, 27.

27. Lippens, G.; Najib, J.; Wodak, S. J.; Tartar, A., Biochemistry 1995, 34, 13-21.

28. Butte, P. V.; Mamelak, A.; Parrish-Novak, J.; Drazin, D.; Shweikeh, F.; Gangalum, P. R.; Chesnokova, A.; Ljubimova, J. Y.; Black, K., Neurosurg. Focus 2014, 36, E1.

29. Veiseh, M.; Gabikian, P.; Bahrami, S. B.; Veiseh, O.; Zhang, M.; Hackman, R. C.; Ravanpay, A. C.; Stroud, M. R.; Kusuma, Y.; Hansen, S. J.; Kwok, D.; Munoz, N. M.; Sze, R. W.; Grady, W. M.; Greenberg, N. M.; Ellenbogen, R. G.; Olson, J. M., Cancer Res. 2007, 67, 6882-8.

30. Costa, P. M.; Cardoso, A. L.; Mendonca, L. S.; Serani, A.; Custodia, C.; Conceicao, M.; Simoes, S.; Moreira, J. N.; Pereira de Almeida, L.; Pedroso de Lima, M. C., Mol. Ther. Nucleic Acids 2013, 2, e100.

31. Xiang, Y.; Wu, Q.; Liang, L.; Wang, X.; Wang, J.; Zhang, X.; Pu, X.; Zhang, Q., J. Drug Target 2012, 20, 67-75.

32. Wang, H.; Gu, W.; Xiao, N.; Ye, L.; Xu, Q., Int. J. Nanomedicine 2014, 9, 1433-42.

33. Ojeda, P. G.; Wang, C. K.; Craik, D. J., Biopolymers 2016, 106, 25-36.

34. Cohen-Inbar, O.; Zaaroor, M., J. Clin. Neurosci. 2016.

35. Han, L.; Cai, Q.; Tian, D.; Kong, D. K.; Gou, X.; Chen, Z.; Strittmatter, S. M.; Wang, Z.; Sheth, K. N.; Zhou, J., Nanomedicine 2016.

36. Chen, Z.; Xiao, E. H.; Kang, Z.; Zeng, W. B.; Tan, H. L.; Li, H. B.; Bian, D. J.; Shang, Q. L., Oncol. Rep. 2016, 35, 3059-67.

37. Rothbard, J. B.; Jessop, T. C.; Wender, P. A., Adv. Drug Deliv. Rev. 2005, 57, 495-504.

38. Mitchell, D. J.; Kim, D. T.; Steinman, L.; Fathman, C. G.; Rothbard, J. B., J. Pept. Res. 2000, 56, 318-25.

39. Sundlass, N. K.; Raines, R. T., Biochemistry 2011, 50, 10293-9.

40. Rydberg, H. A.; Matson, M.; Amand, H. L.; Esbjorner, E. K.; Norden, B., Biochemistry 2012, 51, 5531-9.

41. Jobin, M. L.; Blanchet, M.; Henry, S.; Chaignepain, S.; Manigand, C.; Castano, S.; Lecomte, S.; Burlina, F.; Sagan, S.; Alves, I. D., Biochim. Biophys. Acta. 2015, 1848, 593-602.

42. Christiaens, B.; Symoens, S.; Verheyden, S.; Engelborghs, Y.; Joliot, A.; Prochiantz, A.; Vandekerckhove, J.; Rosseneu, M.; Vanloo, B., Eur. J. Biochem. 2002, 269, 2918-26.

43. D'Souza, C.; Henriques, S. T.; Wang, C. K.; Craik, D. J., Eur. J. Med. Chem. 2014, 88, 10-8.

44. Ojeda, P. G.; Chan, L. Y.; Poth, A. G.; Wang, C. K.; Craik, D. J., Future Med. Chem. 2014, 6, 1617-28.

45. Akcan, M.; Stroud, M. R.; Hansen, S. J.; Clark, R. J.; Daly, N. L.; Craik, D. J.; Olson, J. M., J. Med. Chem. 2011, 54, 782-7.

46. Torcato, I. M.; Huang, Y. H.; Franquelim, H. G.; Gaspar, D. D.; Craik, D. J.; Castanho, M. A.; Henriques, S. T., Chembiochem 2013, 14, 2013-22.

47. Henriques, S. T.; Huang, Y. H.; Castanho, M. A.; Bagatolli, L. A.; Sonza, S.; Tachedjian, G.; Daly, N. L.; Craik, D. J., J. Biol. Chem. 2012.

48. Henriques, S. T.; Huang, Y. H.; Rosengren, K. J.; Franquelim, H. G.; Carvalho, F. A.; Johnson, A.; Sonza, S.; Tachedjian, G.; Castanho, M. A.; Daly, N. L.; Craik, D. J., J. Biol. Chem. 2011, 286, 24231-41.

49. Henriques, S. T.; Pattenden, L. K.; Aguilar, M. I.; Castanho, M. A., Biophys J. 2008, 95, 1877-89.

50. Jacoby, D. B.; Dyskin, E.; Yalcin, M.; Kesavan, K.; Dahlberg, W.; Ratliff, J.; Johnson, E. W.; Mousa, S. A., Anticancer Res. 2010, 30, 39-46.

51. Weksler, B. B.; Subileau, E. A.; Perriere, N.; Charneau, P.; Holloway, K.; Leveque, M.; Tricoire-Leignel, H.; Nicotra, A.; Bourdoulous, S.; Turowski, P.; Male, D. K.; Roux, F.; Greenwood, J.; Romero, I. A.; Couraud, P. O., FASEB J. 2005, 19, 1872-4.

52. Ziegler, A., Adv Drug Deliv Rev 2008, 60, 580-97.

53. Wender, P. A.; Galliher, W. C.; Goun, E. A.; Jones, L. R.; Pillow, T. H., Adv Drug Deliv Rev 2008, 60, 452-72.

54. Naik, R. J.; Chandra, P.; Mann, A.; Ganguli, M., J Biol Chem 2011, 286, 18982-93.

55. Wallbrecher, R.; Verdurmen, W. P.; Schmidt, S.; Bovee-Geurts, P. H.; Broecker, F.; Reinhardt, A.; van Kuppevelt, T. H.; Seeberger, P. H.; Brock, R., Cell Mol Life Sci 2014, 71, 2717-29.

56. Nakase, I.; Takeuchi, T.; Tanaka, G.; Futaki, S., Adv Drug Deliv Rev 2008, 60, 598-607.

57. Tunnemann, G.; Martin, R. M.; Haupt, S.; Patsch, C.; Edenhofer, F.; Cardoso, M. C., FASEB J. 2006, 20, 1775-84.

58. El-Andaloussi, S.; Jarver, P.; Johansson, H. J.; Langel, U., Biochem J. 2007, 407, 285-92.

59. Srinivasan, D.; Muthukrishnan, N.; Johnson, G. A.; Erazo-Oliveras, A.; Lim, J.; Simanek, E. E.; Pellois, J. P., PLoS One 2011, 6, e17732.

60. Fischer, R.; Waizenegger, T.; Kohler, K.; Brock, R., Biochim Biophys Acta 2002, 1564, 365-74.

61. Szeto, H. H.; Schiller, P. W.; Zhao, K.; Luo, G., FASEB J. 2005, 19, 118-20.

62. Sims, P. J.; Waggoner, A. S.; Wang, C. H.; Hoffman, J. F., Biochemistry 1974, 13, 3315-30.

63. Hughes, L. D.; Rawle, R. J.; Boxer, S. G., PLoS One 2014, 9, e87649.

64. Soroceanu, L.; Gillespie, Y.; Khazaeli, M. B.; Sontheimer, H., Cancer Res 1998, 58, 4871-9.

65. Otvos, L., Jr.; Wade, J. D., Front Chem 2014, 2, 62.

66. Fosgerau, K.; Hoffmann, T., Drug Discov Today 2015, 20, 122-8.

67. Guidotti, G.; Brambilla, L.; Rossi, D., Trends Pharmacol Sci 2017, 38, 406-424.

68. Lonn, P.; Kacsinta, A. D.; Cui, X. S.; Hamil, A. S.; Kaulich, M.; Gogoi, K.; Dowdy, S. F., Sci Rep 2016, 6, 32301.

69. Wang, C. K.; Stalmans, S.; De Spiegeleer, B.; Craik, D. J., J Pept Sci 2016, 22, 305-10.

70. Penchala, S. C.; Miller, M. R.; Pal, A.; Dong, J.; Madadi, N. R.; Xie, J.; Joo, H.; Tsai, J.; Batoon, P.; Samoshin, V.; Franz, A.; Cox, T.; Miles, J.; Chan, W. K.; Park, M. S.; Alhamadsheh, M. M., Nat Chem Biol 2015, 11, 793-8.

71. Larsen, M. T.; Kuhlmann, M.; Hvam, M. L.; Howard, K. A., Mol Cell Ther 2016, 4, 3.

72. Ali, S. A.; Alam, M.; Abbasi, A.; Undheim, E. A.; Fry, B. G.; Kalbacher, H.; Voelter, W., Toxins (Basel) 2016, 8, 36.

Figure captions

Figure 1. Three-dimensional structure of chlorotoxin and sequences of chlorotoxin and analogues. A. Schematic representation of chlorotoxin (PDB:1CHL) with the backbone colored white. Disulfide bonds and mutated residues are shown in stick format, labeled and colored grey. **B.** Sequence of chlorotoxin (CTX) and its analogues. Residues mutated to produce CTX_M1 and CTX_M2 are boxed. The disulfide bond connectivity of CTX and its analogues is shown at the bottom of the figure and the cysteines are numbered using Roman numerals.

Figure 2. Characterization of structure, stability and cytotoxicity of chlorotoxin and analogues. A. The similar αH chemical shift values of chlorotoxin (CTX; circle) and the analogues, CTX_M1 (inverted triangle) and CTX_M2 (diamond), show that they adopt similar folds. **B.** The percentage of peptide remaining after a 24-h incubation in human serum at 37°C. The amount of peptide remaining was calculated by comparing the height of the elution peak of peptides incubated in human serum and that of peptides that had not been incubated. **C.** Cytotoxicity of CTX and its analogues to HeLa cells after a 1-h incubation. Cell viability was determined by the MTT assay. Controls with buffer and Triton X-100 at 0.01% (v/v) were used to establish 100% and 0% of cell survival, respectively. Data points are shown as mean ± SD of three experiments.

Figure 3. Internalization of fluorescently labeled peptides into HeLa cells, as measured by flow cytometry. A. Internalization of peptides labeled with Alexa Fluor® 488 at 37°C**. B.** Internalization of peptides labeled with Cy5.5™ at 37°C. **C.** Internalization of peptides labeled with Alexa Fluor® 488 at 4°C. **D.** Internalization of peptides labeled with Cy5.5™ at 4°C. The

mean fluorescence emission intensity of 10,000 cells was measured at 488 nm for cells treated with Alexa Fluor® 488-labeled peptides and at 633 nm for cells treated with Cy5.5™-labeled peptides. Data are represented as mean ± SD of at least two independent experiments. The statistical analysis was performed using an ANOVA Tukey's multiple comparisons test by comparison of CTX_M1 and CTX_M2 with CTX (****$p < 0.001$). Relative fluorescence emission intensity was normalized to TAT at 37°C.

Figure 4. Confocal microscopy images of live HeLa cells treated with fluorescently labeled peptides. Cells were incubated at 37°C for 1 h with Cy5.5™-labeled CTX (**A**), CTX_M1 (**B**) and CTX_M2 (**C**) or with Alexa Fluor® 488-labeled CTX (**D**), CTX_M1 (**E**), and CTX_M2 (**F**). Magnification of the cells is also shown (inset).

Figure 5. Interaction of peptides with POPC model membranes, studied by SPR. Binding of CTX (**A**), CTX_M1 (**B**) and CTX_M2 (**C**) to POPC bilayers deposited onto an L1 chip. Sensorgrams were obtained upon injection of 25 µM, 50 µM, 100 µM and 200 µM of peptide over POPC bilayer over time, as indicated in panel **(A)**. Peptides were injected for 180 s and dissociation followed for 800 s. The response signal was normalized and represented as P/L (peptide-to-lipid ratio) versus time. Despite evidence of some binding, when the membrane affinities shown in this figure are compared with the affinities of other peptides that we have previously characterized, for example kalata B1 or TAT,[20, 47] the lipid affinity of CTX and its analogues is low.

Figure 6. Interaction of labeled and unlabeled peptides with POPC/POPS model membranes, studied by SPR. A. Comparison of the affinity of unlabeled peptides or labeled with Alexa Fluor® 488 (CTX and CTX_M1) for POPC/POPS membranes. **B.** Comparison of the affinity of unlabeled peptides or labeled with Cy5.5™ (CTX and CTX_M1) for POPC/POPS membranes. The response signal was normalized and represented as P/L (peptide-to-lipid ratio) versus time.

Figure 1

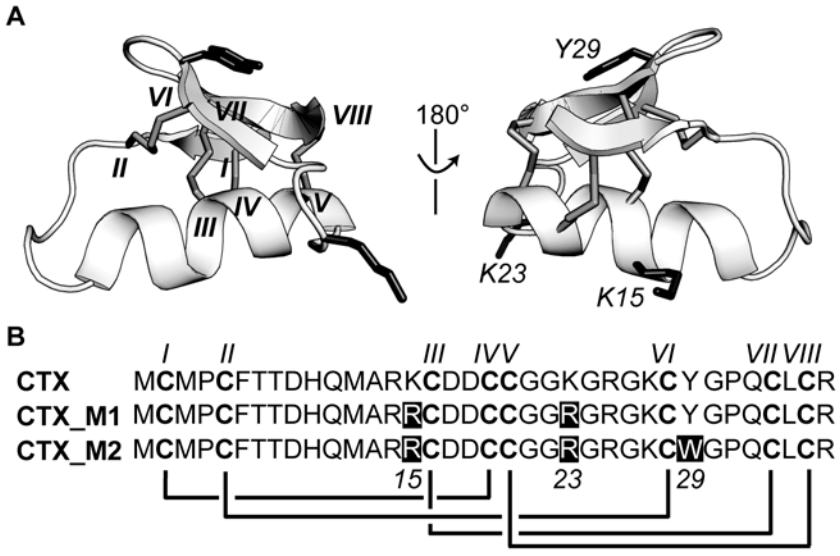
A
VI
VII
VIII
II
I
IV
V
III
180°
Y29
K23
K15
B
I II III IVV VI VII VIII
CTX MCMPCFTTDHQMARKCDDCCGGKGRGKC Y GPQCLCR
CTX_M1 MCMPCFTTDHQMARRCDDCCGGRGRGKC Y GPQCLCR
CTX_M2 MCMPCFTTDHQMARRCDDCCGGRGRGKCWGPQCLCR
15
23
29

Figure 2

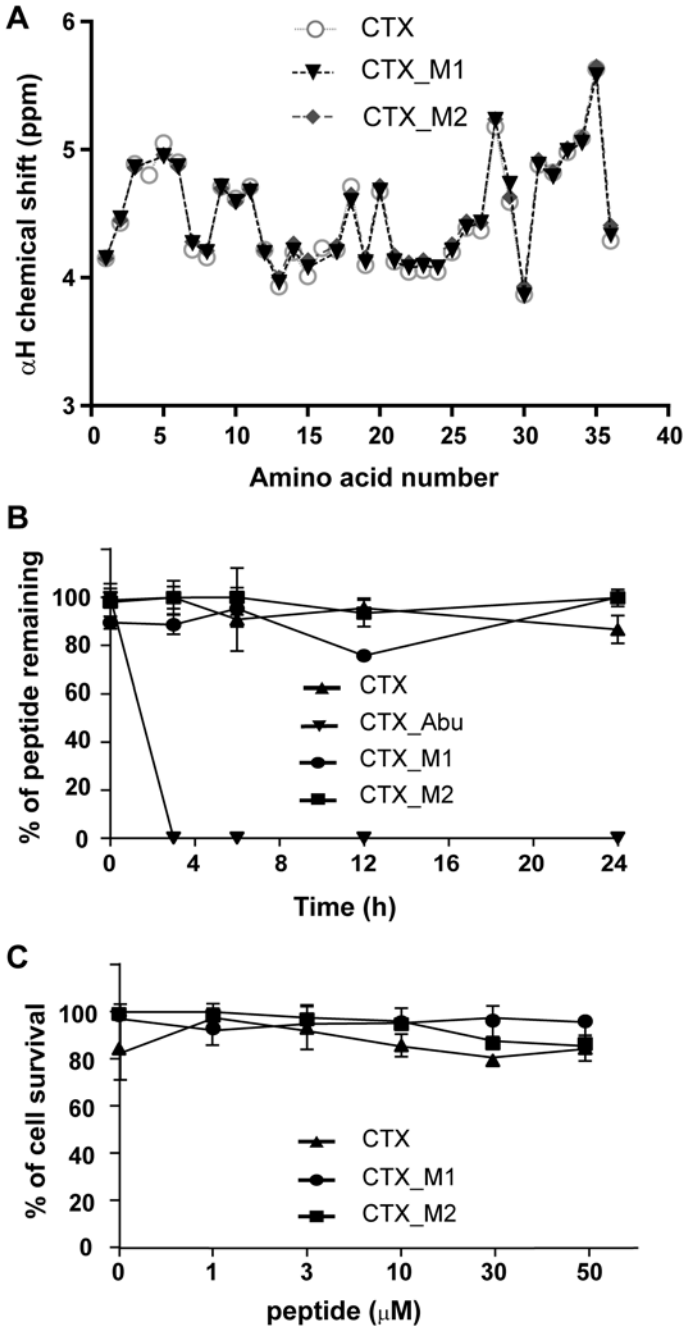
A
CTX
CTX_M1
CTX_M2
αH chemical shift (ppm)
Amino acid number
B
% of peptide remaining
CTX
CTX_Abu
CTX_M1
CTX_M2
Time (h)
C
% of cell survival
CTX
CTX_M1
CTX_M2
peptide (μM)

Figure 3

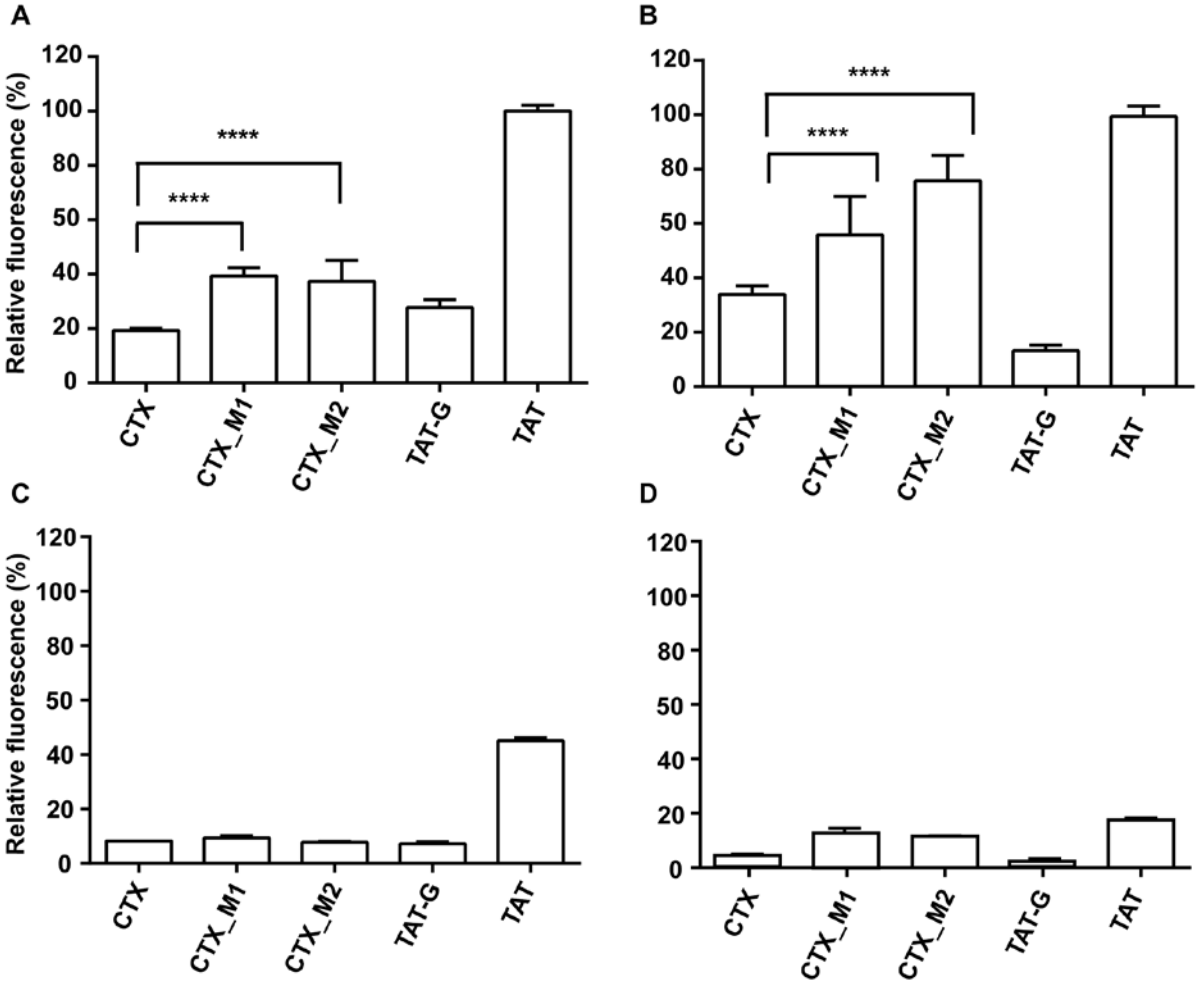
A
B
C
D
Relative fluorescence (%)
120
100
80
50
40
20
0
****
****
CTX
CTX_M1
CTX_M2
TAT-G
TAT

Figure 4

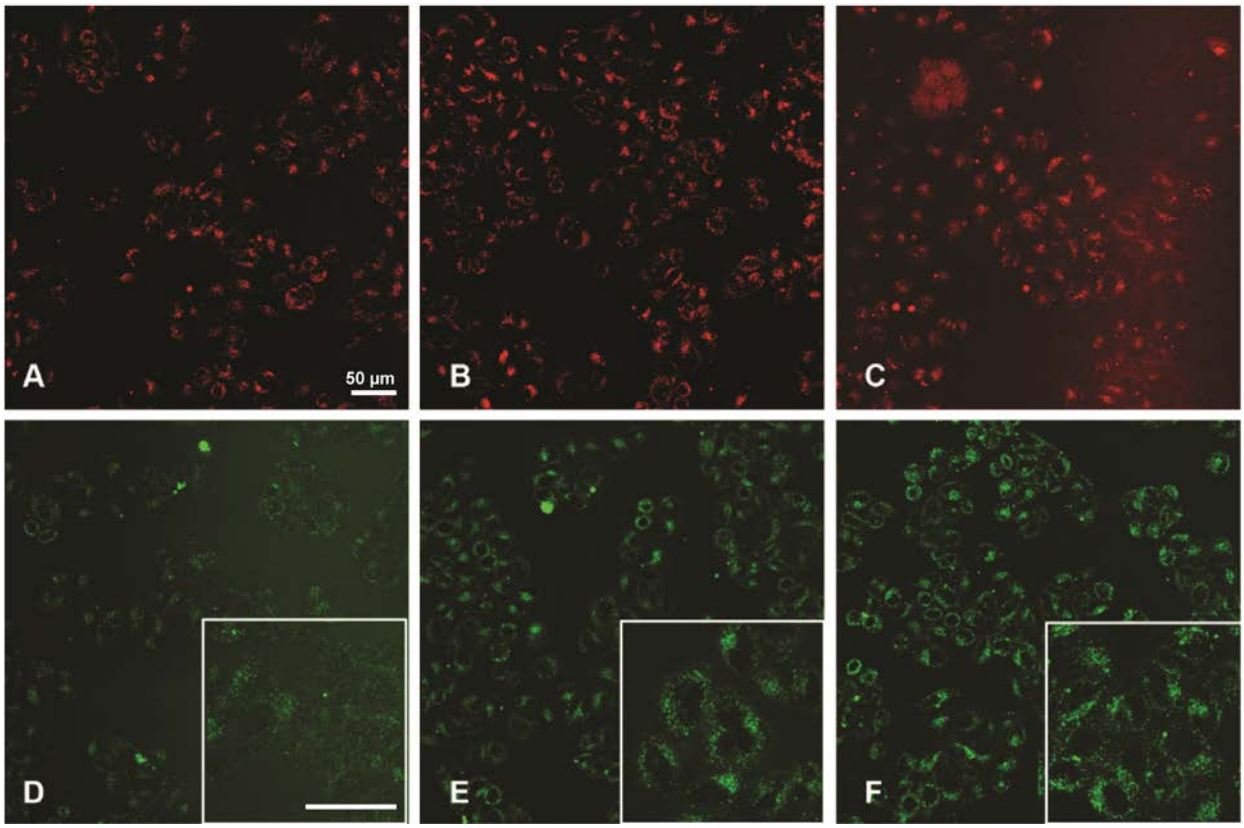

Figure 5

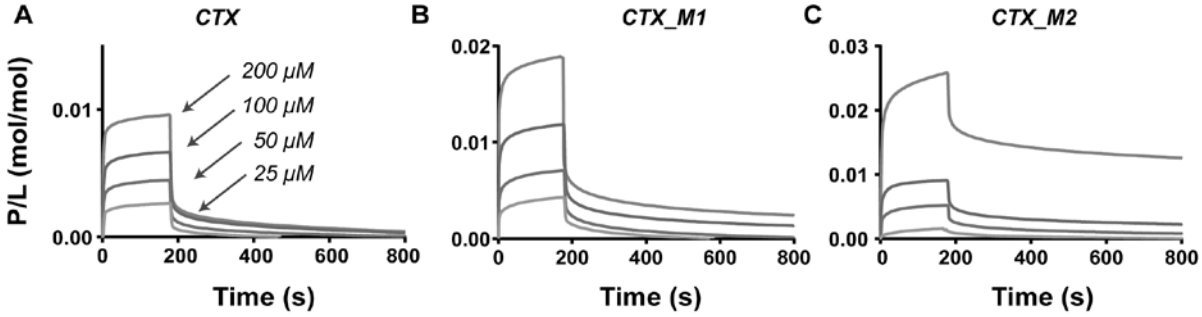
A
CTX
200 µM
100 µM
50 µM
25 µM
P/L (mol/mol)
0.01
0.00
0
200
400
600
800
Time (s)
B
CTX_M1
0.02
0.01
0.00
0
200
400
600
800
Time (s)
C
CTX_M2
0.03
0.02
0.01
0.00
0
200
400
600
800
Time (s)

Figure 6

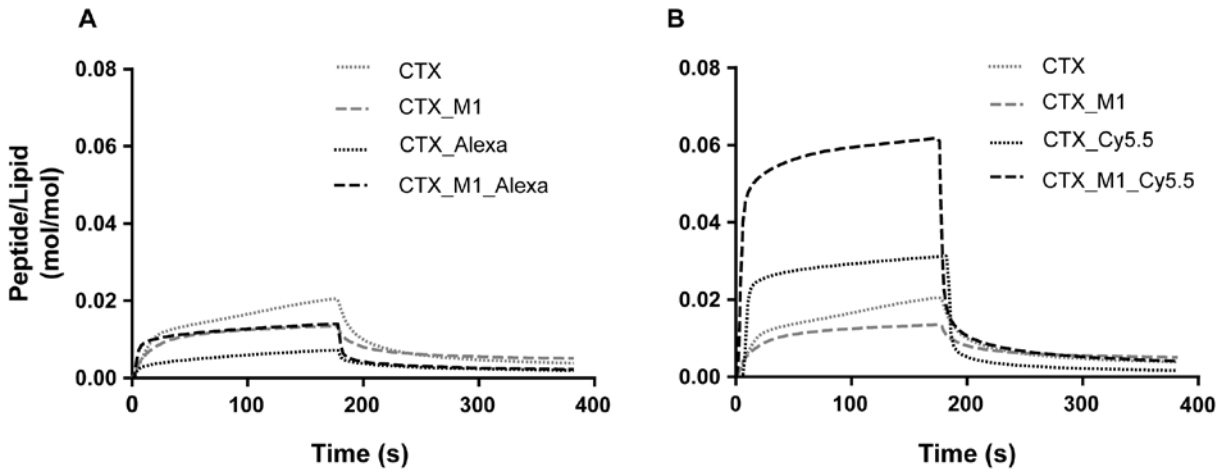
A
B
Peptide/Lipid (mol/mol)
0.08
0.06
0.04
0.02
0.00
0
100
200
300
400
Time (s)
CTX
CTX_M1
CTX_Alexa
CTX_M1_Alexa
CTX_Cy5.5
CTX_M1_Cy5.5

For Table of Contents Use Only

Title: Lysine to arginine mutagenesis of chlorotoxin enhances its cellular uptake

Authors: Paola G. Ojeda, Sónia Troeira Henriques, Yijun Pan, Joseph A. Nicolazzo, David J. Craik and Conan K. Wang·